Journal of Hazardous Materials 215–216 (2012) 266–271

Contents lists available at SciVerse ScienceDirect

Journal of Hazardous Materials

journal homepage: www.elsevier.com/locate/jhazmat

Cerium(III) molybdate nanoparticles: Synthesis, characterization and radionuclides adsorption studies

Taher Yousefi[a,b,*], Ali Reza Khanchi[a,*], Seyed Javad Ahmadi[a], Mohamad Kazem Rofouei[b], Ramin Yavari[a], Reza Davarkhah[a], Behzad Myanji[a]

[a] NFCRS, Nuclear Science and Technology Institute, Kargher Ave, Tehran, Iran
[b] Tarbiat Moallem University, Mofatteh Ave, Tehran, Iran

ARTICLE INFO

Article history:
Received 17 October 2011
Received in revised form 3 February 2012
Accepted 25 February 2012
Available online 3 March 2012

Keywords:
Nanoparticles
Cerium(III) molybdate
Ion-exchange capacity
Cesium radionuclide

ABSTRACT

Cerium(III) molybdate nanostructure with average size about 40 nm was prepared by adding cerium(III) chloride and ammonium molybdate solutions under varying conditions. The product was characterized by X-ray diffraction (XRD), scanning electron microscopy (SEM), transmission electron microscopy (TEM), Fourier transform infrared (FT-IR), thermogravimetric analysis (TGA) and Brunauere Emmette Teller (BET) techniques. Ion exchange capacity of the sample for potassium ion and distribution coefficients (K_d) for 23 metal ions were determined, the K_d values for Tl(I), Pb(II), Th(IV), U(VI), and Cs(I) ions were found to be sufficiently high for their removal from various effluents. The adsorption behavior of the sample towards $Cs(I)_{134}$ species were studied. Finally, the binary separation of Dy(III)–U(VI), Sm(III)–Th(IV) and Cs(I)–Rb(I) and removal of $Cs(I)_{134}$ from the real sample were successfully achieved.

1. Introduction

Due to the growing concern for the release of industrial liquid effluents in the environment, the waste management emerges as one of the most challenging areas of new research [1–4]. In this field of research, one of the aims is to reduce the volume of liquid wastes to be disposed. In recent years, increased attention has been focused on the development of new separation methods in order to resolve concerning problems. Among them, ion exchange methods have played an important role in the dissemination of the chemical analysis, purification, concentration, preconcentration and recovery techniques for ionic species from aqueous as well as non-aqueous systems [5–7]. Inorganic ion exchange materials are one of the important groups of the used materials for the recovery of metal ions and confinement of different radionuclide (high, medium and low-lived) from nuclear effluents because of their resistance to oxidation, excellent stability towards thermal and radiation doses as well as more compatibility with cement containment [8–11]. The inorganic nanostructures have received considerable attention to solve environmental problems because of their novel properties, which differ from those of bulk materials. The inorganic nanostructures possess the advantages of large surface area and high number of surface active sites, which lead to high adsorption efficiency, high removal rate of contaminants. [12]. Moreover, due to the high selectivity of these nanostructures in certain metal ions, more attention has been paid to their ability for removal of toxic heavy metals such as Hg(II), Pb(II), Tl(I), and Bi(III) from the environmental waste. Hence, an extended attempt is now made on the development of new ion exchanger nanostructures [13–17]. In the present study, new cerium(III) molybdate nanostructure has been prepared. It was characterized and applied to the binary separation. Finally, the potential use of the ion exchanger for uptake of cesium ions was also examined.

2. Experimental

2.1. Reagents

All chemicals were of analytical grade (E. Merck or Aldrich) and used without further purification.

2.2. Apparatus

Thermogravimetric analysis was performed on a thermobalance (PL-STA 1500, PL Thermal Science). The pH measurements were made with a Schott CG841 pH-meter (Germany). Bruker Spectrometer (Vector 22) was employed for IR studies. The quantitative determinations of inorganic ions were performed by an inductively coupled plasma ((ICP) Varian Turbo (Model 150-Axial Liberty). Atomic absorption spectrometer (AAS Model, Spectra

* Corresponding authors at: NFCRS, Nuclear Science and Technology Institute, Kargher Ave, Tehran, Iran. Tel.: +98 9124865930.
E-mail address: Taher_yosefy@yahoo.com (T. Yousefi).

0304-3894/$ – see front matter © 2012 Elsevier B.V. All rights reserved.
doi:10.1016/j.jhazmat.2012.02.064

Table 1
The synthesis conditions and ion exchange capacities of various cerium(III) molybdate.

Sample	CC (M)	AM (M)	Mixing ratio (v/v)	pH	Appearance	Ion-exchange capacity
S-1	0.025	0.025	1:1	5	Yellow	0.85
S-2	0.025	0.025	2:1	3.4	Pale yellow	0.49
S-3	0.050	0.050	1:1	5.4	Light yellow	1.45
S-4	0.050	0.050	2:1	4.2	Yellow	1.10

CC, cerium(III) chloride; AM, ammonium molybdate.

AA-220 Varian), and the morphology of the sample were studied by scanning electron microscopy (LEO 1455VP) and transmission electron microscopy (TEM, Phillips EM 2085). A gamma spectrometer (Ortec EG&G, HPGe) comprising of a high-resolution coaxial GMX detector with 4096 channels and an Alpha-Counter (Model LB-770) were used. X-ray diffraction studies were made with a Jeol X-ray diffractometer (model GDX-8030 Japan, Cu Kα). The measurement of specific surface area for the prepared sample was performed through measuring N_2 adsorption–desorption isotherms at 77 K with a Quanta-chrome NOVA-2200e system, and a water-bath shaker (model CH-4311, Infors AG) for equilibrium examination was used throughout the work.

2.3. Synthesis of cerium(III) molybdate nanostructures

Four different types of cerium(III), molybdates were synthesized by the gradual addition of ammonium molybdate solution to cerium(III) chloride solution with continuous stirring in different volume ratios under varying concentration conditions, the result of which is given in Table 1. The pHs of solutions were adjusted by the addition of either HNO_3 or NaOH along with regular shaking at room temperature. After completion of the reaction, the yellow precipitate obtained was allowed to settle for 24 h. The supernatant was separated and the precipitate was washed several times with demineralized water (DMW) until the filtrate pH was 6.5–7. It was then filtered and dried in an air oven at 70 °C. The material was finally converted into H^+ form.

3. Characterization and application

3.1. Ion-exchange capacity (IEC)

1 g of the adsorbent in H^+ form was poured into a glass chromatographic column with an interval diameter of 0.8 cm filled with glass wool at the bottom. 100 ml from 1 M of KCl was passed slowly through the column at a flow rate of 0.3 ml/min. The effluent was carefully collected. For completion of the replacement of H^+ ions with adsorbent, a pH paper was used. The elute containing librated acid was estimated by titration with standard alkali solution. The value of ion-exchange capacity is represented in Table 1.

3.2. Composition of cerium(III) molybdate

0.05 g of each sample was dissolved in (30 ml) hot concentrated HNO_3 and HCl. The Ce(III) and Mo were determined by ICP. The results are shown in Table 2.

Table 2
Composition of cerium(III) molybdates.

	S-1	S-2	S-3	S-4
Ce (mg)	12.70	10.70	1.12	10.25
Mo (mg)	22.50	21.50	21.70	21.20
MO/Ce ratio	1.95	2.01	1.97	2.02

Table 3
Chemical dissolution of cerium(III) molybdate in different concentrations of acids and alkali.

Type of solvent	Ce (mg/L)	Mo (mg/L)
0.5 M HNO_3	0.0	0.0
1 M HNO_3	1.3	2.6
4 M HNO_3	3.0	6.0
0.5 M HCl	0.0	0.0
1 M HCl	1.0	2.0
4 M HCl	2.5	5.2
0.5 M NaOH	0.0	0.0
1 M NaOH	0.0	0.0
4 M NaOH	2.9	5.7
Acetone	0.0	0.0
Ethanol	0.0	0.0
Methanol	0.0	0.0
DMW	0.0	0.0

3.3. Chemical stability

The chemical stability of each sample was assessed in mineral acids (HCl and HNO_3), base (NaOH), water and organic solvents (acetone, methanol and ethanol). 0.05 g of each sample was placed in a glass test tube containing 20 ml of the interested solvent and was kept for 24 h with continuous shaking at room temperature. For determining the amount of dissolved ion exchanger, ICP technique was used (Table 3).

3.4. Distribution coefficients

Distribution coefficients (K_d) for twenty three metal ions that are Tl(I), Li(II), Na(I), K(I), Cs(I), Rb(I), Sr(II), Be(II), Zn(II), Pb(II), Dy(III), Sm(III), Nd(III), La(III), Cr(III), Cr(VI), Zr(IV), Hf(IV), UO_2(II), Th(IV), Fe(II), Cd(II) and Sb(VI) ions were determined in aqueous solutions by the batch method using the following formula:

$$K_d = \frac{I - F}{F} \times \frac{V}{M}$$

where I is the initial amount of the metal ion in the solution, F is the final amount of the metal ion in solution, V (ml) is the volume of the metal ion in solution and W (g) is the weight of the ion exchanger. The exchanger (0.2 g) in H^+ form was equilibrated with mixing 19.5 ml of DMW and 0.5 ml of 0.005 M solution of the metal ion in a plastic bottle. It was shaken at 25 °C for 5 h, and the concentration of metal ion was determined in the filtrate using ICP technique (Table 4). With regard to the ion exchange capacity and distribution coefficients (especially for the Cs^+) the sample 3 (S-3) was selected for further analysis and separation application.

3.5. SEM and TEM

The size and morphology of the sample (S-3) were examined by SEM and TEM. The results are shown in Fig. 1(a)–(d).

3.6. Infrared absorption spectra

Infrared spectrum of sample (S-3) was provided by the standard disc technique in H^+ form (Fig. 2). 10 mg (dry mass) of each material (H^+ form) was taken, and the ion exchange material was then thoroughly mixed with 0.5 g (dry mass) of KBr and ground to a very fine powder. A transparent disc was formed by applying a high pressure in a moisture-free atmosphere. The diameter of the transparent disc was about 1.2 cm. The IR absorption pattern recorded was between 200 and 4500 cm^{-1}.

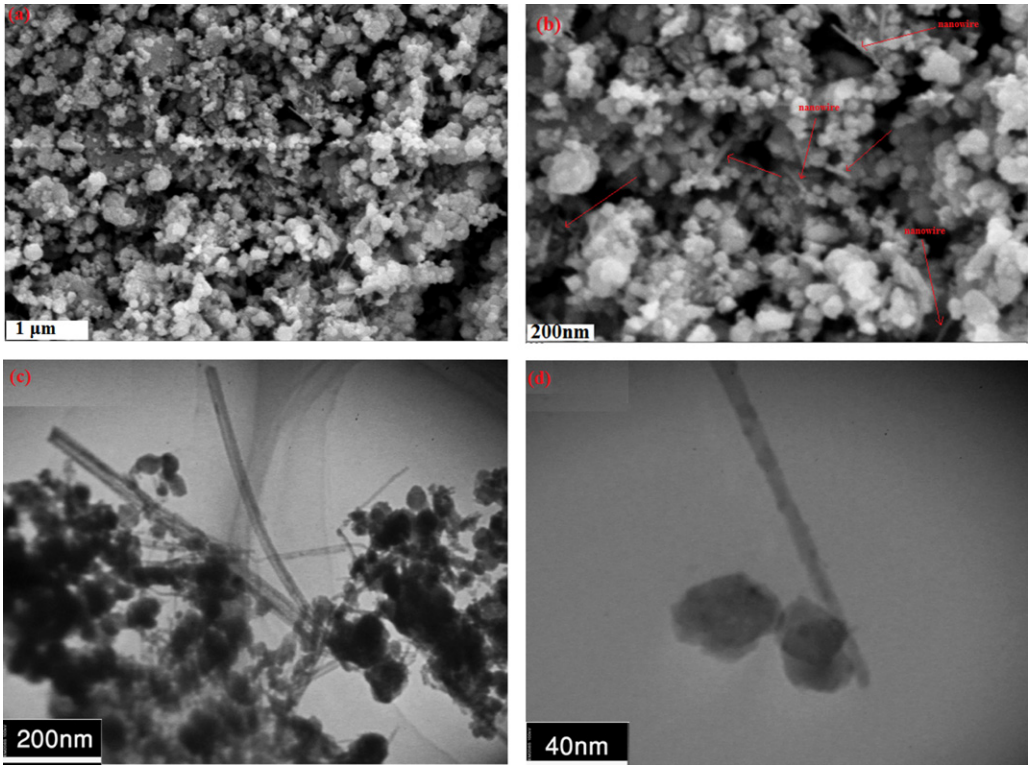

Fig. 1. SEM and TEM images of sample (S-3).

3.7. X-ray diffraction, thermogravimetric and BET analysis

For thermal analysis investigation, 0.1 g of the sample (S-3) in H^+ form was analyzed (from ambient temperature to 1000 °C), the thermogravimetric analysis of the sample was performed at a heating rate of 10 °C/min. The thermogram for the sample 3 in H^+ form is recorded in Fig. 3. For X-ray diffraction (XRD) analysis, nickel filtered Cu-Kα radiations were used. The N_2 adsorption–desorption analysis was used for surface area and pore size determination.

Table 4
Distribution coefficients of metal ions on different types of cerium(III) molybdates (ml g^{-1}).

Metal ions	S-1	S-2	S-3	S-4
Li(I)	NA	NA	NA	NA
Na(I)	NA	NA	NA	NA
K(I)	101	47	190	120
Cs(I)	438	259	3.6×10^3	284
Rb(I)	583	117	158	74
Sr(II)	29	35	88	28
Be(II)	8	9	9	2
U(VI)	682	477	768	912
Th(IV)	778	635	1.1×10^3	1.2×10^3
Sm(III)	41	26	36	32
Dy(III)	28	37	30	28
Nd(III)	214	249	207	218
La(III)	122	196	152	16
Tl(I)	3×10^3	1×10^3	3×10^3	2×10^3
Zn(II)	4	NA	NA	3
Pb(II)	7.1×10^4	5.9×10^5	8.2×10^4	6.2×10^5
Cr(III)	6	10	5	3
Cr(VI)	8	6	5	10
Zr(IV)	7.9×10^4	1.8×10^5	3.9×10^4	1.8×10^4
Hf(IV)	6×10^3	3×10^3	3×10^3	5×10^3
Fe(II)	130	42	139	118

NA, negligible adsorption.

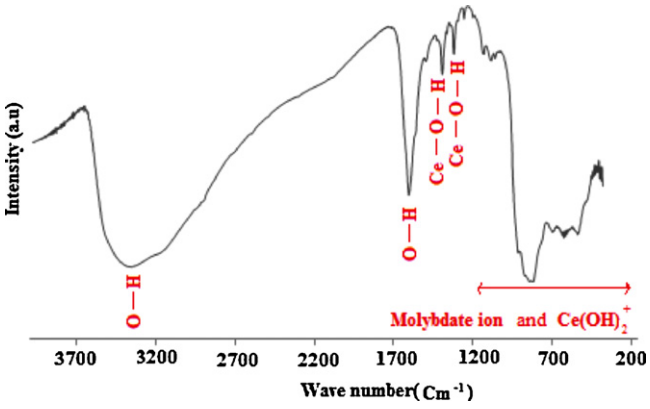

Fig. 2. IR spectrum of cerium(III) molybdate (S-3) in H^+ form.

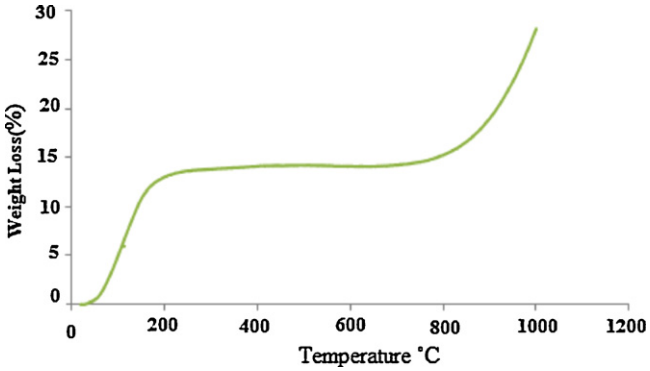

Fig. 3. Thermogram of cerium(III) molybdate (S-3) in H^+ form.

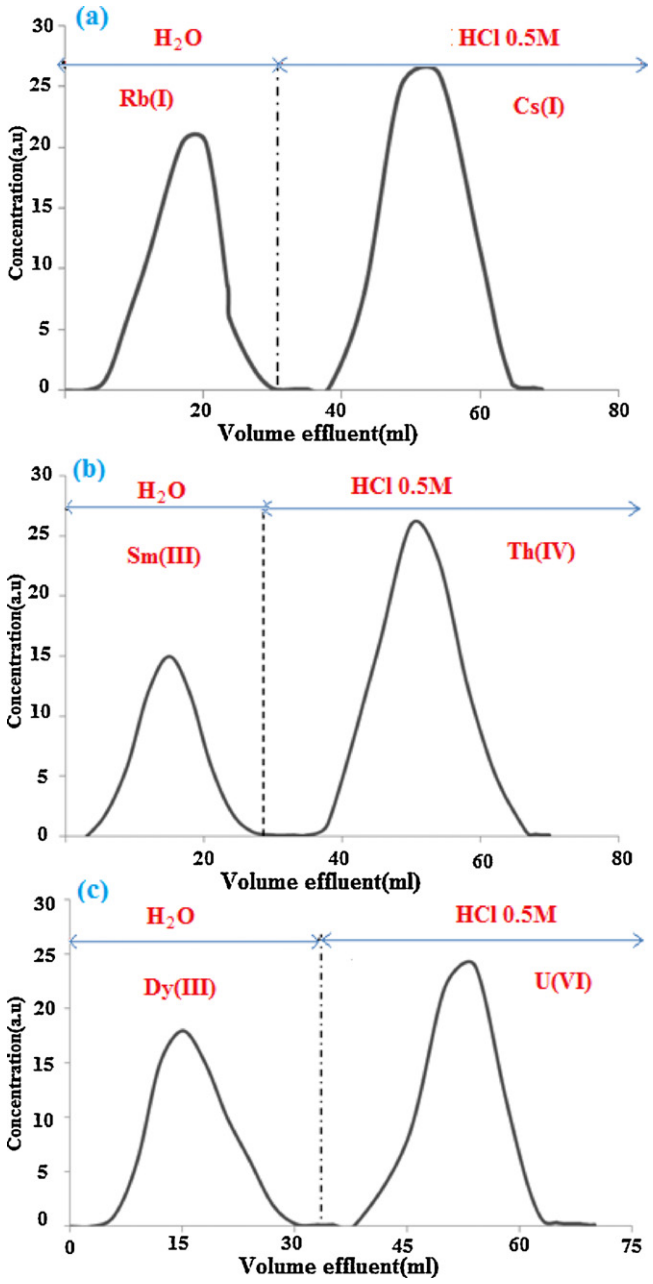

Fig. 4. Elution curve of separation of (a) Rb(I)–Cs(I), (b) Sm(III)–Th(IV), and (c) Dy(III)–U(VI) flow rate of the eluent; 0.3 ml/min.

3.8. Binary separation of metal ions

A slurry of 1 g of cerium(III) molybdate in H^+ form was poured in a glass column with a bore of 0.8 cm after pretreatment of column with DMW, with mixing 0.5 ml of 0.005 M from each of Dy(III) and UO_2(II) ions, and total volume of solution was reached 4 ml with DMW. The metal ion mixture was then added to the column. The Dy^{3+} ion was eluted by DMW while for elution of uranyl ions 0.5 M HCl was used. The flow rate of the eluent was maintained at 0.3 ml/min throughout the procedure. The results of quantitative separations are shown in Fig. 4. The separation conditions of Sm(III)–Th (IV) and Cs(I)–Rb(I) systems were similar to those of Dy(III) and UO_2(II) ions. Their chromatograms are shown in Fig. 4(a)–(c).

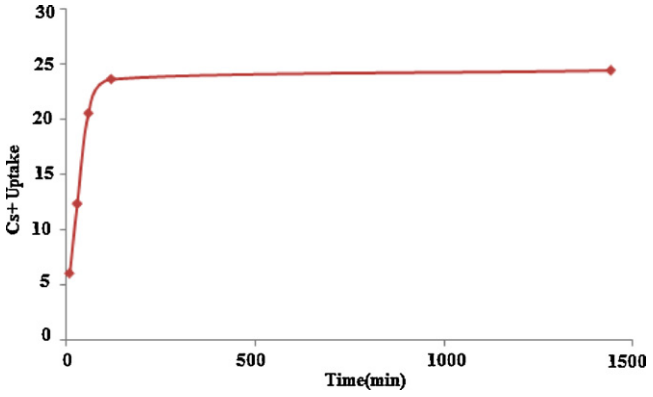

Fig. 5. Kinetics study of Cs^+ on cerium(III) molybdate.

3.9. Kinetics of Cs(I) sorption

Adsorption kinetics of Cs(I) ion onto cerium(III) molybdate (S-3) were investigated by placing 0.05 g of the sample with 10 ml of the metal ion in 0.005 M concentration into each plastic bottle. Then the bottles were shaken and adjusted at an ambient temperature at different time intervals. The supernatant was separated from the adsorbent and then analyzed by ICP spectroscopy (Fig. 5).

3.10. The effects of interfering ions

A number of simulated nuclear liquid wastes were prepared in which the other alkali metal ions were added. For this purpose, cesium ion uptake in the presence of Na^+(NaOH), K^+(KOH) and H^+(HCl) in the concentration ranges from 1×10^{-3} to about 2 M was examined by the batch method at ambient temperature. In all these cases the contact time was 5 h. The final concentration of all tested metal ions was measured by atomic absorption spectroscopy. The affinity of the exchanger for Cs(I) was expressed through the distribution coefficient (Fig. 6).

3.11. Effect of pH on Cs(I) adsorption and removal of $Cs(I)_{134}$ from nuclear waste

Because of the various pH values of nuclear wastes the pH effect on the removal of $Cs(I)_{134}$ in the range of 0.5–11 was examined. The ion exchanger (S-3, 0.2 g) in H^+ form was equilibrated with mixing 19.5 ml of DMW and 0.5 ml of 0.005 M solution of $Cs(I)_{134}$ ion in a plastic bottle for 2 h then the cesium concentration was determined by γ-ray spectroscopy (Fig. 7). Finally, in order to determine Cs uptake of the ion exchanger in the real sample, an aliquot part of

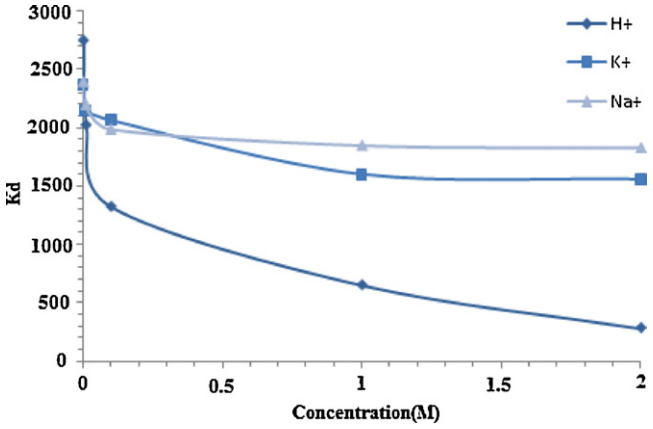

Fig. 6. The effect of Na^+, K^+ and H^+ on the uptake of Cs^+ by cerium(III) molybdate.

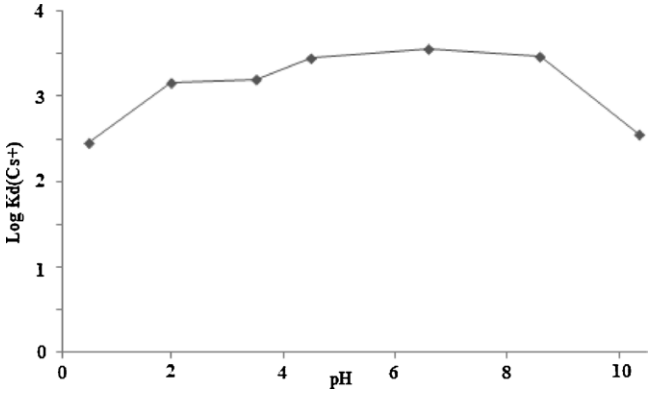

Fig. 7. The effect of pH on the uptake of Cs^+ by sample.

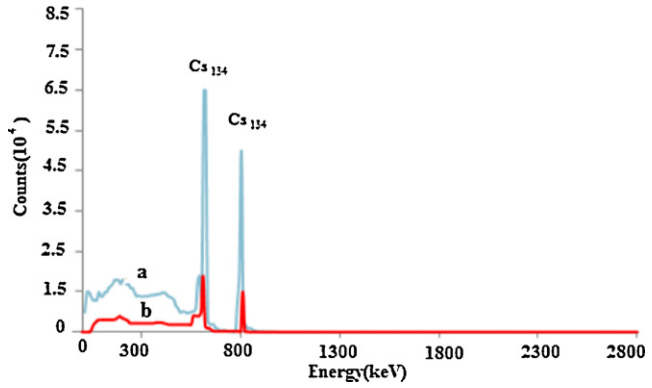

Fig. 8. Gamma spectra of Tehran reactor waste pool solution before (a) and after (b) treatment with sample.

the waste pool of Tehran reactor equilibrated with ion exchanger in batch experiment for 2 h was then analyzed by γ-ray spectroscopy (Fig. 8).

3.12. Titration of ion exchanger

Cerium(III) molybdate (0.2 g) was placed in a column that was fitted with glass wool at its bottom. A glass bottle containing 20 ml of 0.001 M HCl was placed below the column, and for determination of pH, a glass electrode was placed in the solution, then 60 ml of NaOH was poured into the column. Titration was carried out, by passing the NaOH solution at a drop rate of about 0.3 ml/min, and continued to a pH of about 13 (Fig. 9).

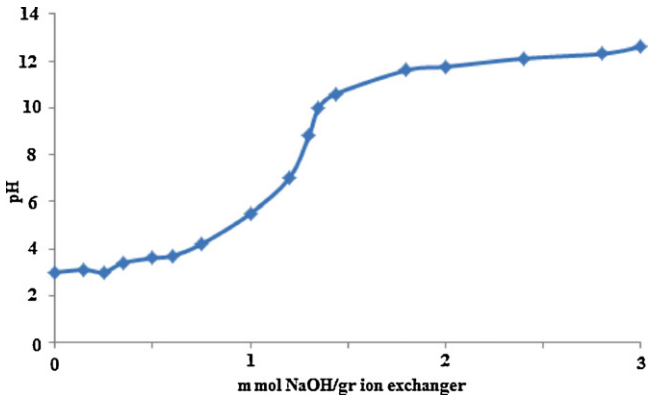

Fig. 9. pH titration curve for cerium(III) molybdate.

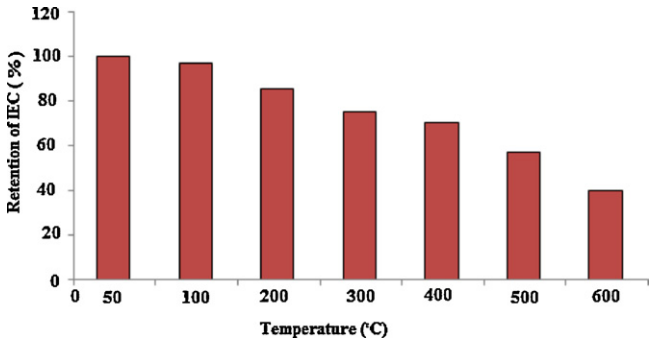

Fig. 10. Effect of temperature on ion-exchange capacity cerium(III) molybdate.

3.13. Thermal effect on ion exchange capacity

To study the effect of temperature on the ion exchange capacity, 0.5 g sample of the prepared ion exchange materials in the H^+ form were heated at various temperatures in furnace for 1 h and the ion exchange capacity after cooling to room temperature was determined by the column process (Fig. 10).

4. Results and discussion

SEM images show (Fig. 1a) that the samples are composed of very different particle sizes ranged from 10 to 60 nm. Moreover, a close examination reveals that the fine nanowires with average diameter of 10 nm can be seen among nanoparticles (Fig. 1b). This combination morphology can increase specific surface area of the sample and it is in line with BET results. The TEM images (Fig. 1c and d) are consistent with SEM images and further confirm the complex morphology of the sample.

The IR curve of cerium molybdate (Fig. 2, S-3) shows a broad band in the region of 2900–3700 cm^{-1}, a sharp peak in 1632, 1400 and 1340 cm^{-1}, and a broad band in the region of 500–800 cm^{-1}. The peak at 2900–3700 and 1632 cm^{-1} are characteristics of O–H stretching and bending modes. The first peak between 2900 and 3700 cm^{-1} with a maximum of 3421 cm^{-1} is due to interstitial water (or lattice water) [18] while the smaller sharp peaks at 1400 and 1340 cm^{-1} are due to M–O–H bending mode which shows the presence of Ce–O–H, the board peak in this compound at 550–900 cm^{-1} corresponds to the overlapping of the bands of molybdate ion and $Ce(OH)^{2+}$[19]. A small band between 1050 and 1070 cm^{-1} corresponds to the metal–oxygen bonds in the molybdate ion. The XRD patterns of powder for S-3 (not shown) indicate that the sample was amorphous and noncrystalline in nature. The results of the N_2 adsorption–desorption analysis indicated that the BET surface area of the sample 2 is 79.2 $m^2\,g^{-1}$ and the pore size distribution is 4 nm. With regard to the IUPAC classification, the sample belongs to the mesopore group. According to IUPAC nomenclature, micropores are less than 2 nm in diameter, mesopores are between 2 and 50 nm in diameter, and macropores are greater than 50 nm in diameter [20].

The thermogram of S-3 in H^+ form which is given in Fig. 3 can be explained as follows: the weight loss of the ion exchanger up to 180 °C is due to the removal of free external water molecules. Its thermal stability is constant up to 850 °C. Then it is rapidly decomposed due to the formation of cerium and molybdenum oxide and sublimation of molybdenum oxide consequently [19].

As is shown in Table 1, the concentration of the reactants used in the synthesis of the exchanger has a considerable effect on the ion exchange capacity. With increasing reactant concentration from 0.025 mol to 0.050 mol, higher ion exchange capacity is achievable, but no regular trend is observed in the ion exchange capacity with variation of pH at the final step (after precipitation). Based

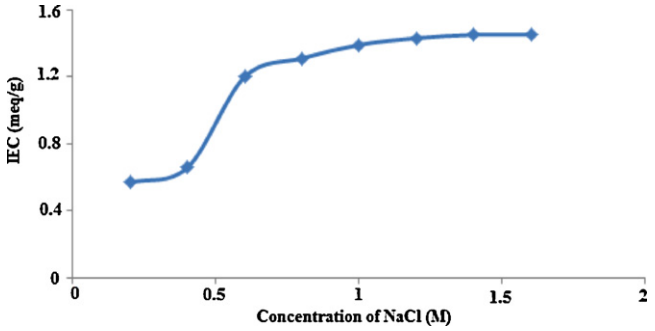

Fig. 11. Exchange capacity of cerium(III) molybdate as a function of eluent concentration.

on the obtained results of Table 2 the Ce:Mo ratio of the samples is about 0.5. The chemical stability investigation results show that the exchanger is apparently stable in water, organic solvents, nitric and hydrochloric acids and sodium hydroxide solutions (Table 3).

K_d values in Table 4, denote that the exchanger is capable of high selectivity in some toxic and radioactive metal ions: Pb(II), Tl(II), U(VI), Zr(IV) and Hf(IV). On the basis of the K_d values, some lanthanide metal ions, Dy(III) and Sm(III), are separated from actinide metal ions [U(VI) and Th(IV)] by column experiments (Fig. 4a and c). Samarium and dysprosium can be conveniently separated from thorium and uranium ions by demineralized water, while under these conditions, uranium and thorium are totally adsorbed by the ion exchanger. Rubidium can also be separated from cesium by mobile phase and cesium ion can consequently be transferred to the outside of the column by 0.5 M HCl (Fig. 4a).

The study of uptake rate for cesium ion shows that its reaction with the ion exchanger is fairly rapid in the ppm concentration ranges under vigorously shaking conditions (150 rpm). Under these conditions, the film diffusion mechanism can be eliminated or reduced. Cesium ion attains equilibrium with cerium molybdate in less than 20 min (Fig. 5).

As is illustrated in Fig. 6, the variation of two alkali metal ion concentrations have minimal effects on the sorption of cesium ions, so that in the concentration of 2 mol of alkaline ions, the reduced amount of K_d value is less than 15% for each of the ions. But considering the acidic medium, with increasing acid concentration, sorption of the cesium ions decreases markedly compared with alkaline ions, and the value of K_d variation except for 2 mol HNO_3 is not considerable. The results of γ-ray spectroscopy for the pH effect on Cs(I) uptake (Fig. 7) clearly illustrated the suitable pH area for Cs(I) uptake ranged from 3 to 8. With a lower pH, the H^+ compete with Cs(I) ion and with a higher pH, slight dissolution of the ion exchanger reduces Cs(I) uptake. So as predicted, $Cs(I)_{134}$ was successfully removed from nuclear waste and can be seen in Fig. 8, that waste activity was reduced to lower than 15% after equilibration with ion exchanger (note: the ^{134}Cs has two peaks at 604 keV and 795 keV). Fig. 9 shows the pH–titration curve of the cerium(III) molybdate. The pH of solution was measured and plotted against milliequivalents of OH ions. The pH titration curve shows only one inflexion point indicating that the cerium(III) molybdate behaves as monofunctional. The results of thermal effect on ion exchange capacity studies are shown in Fig. 10. The ion exchange capacity of cerium(III) molybdate is affected by drying temperature. As the drying temperature of the material increases ion-exchange capacity decreases. It retains about 80% of its initial ion exchange capacity by heating up to 200 °C. The effect of the concentration of NaCl (Fig. 11) on exchange capacity of this compound shows a constant capacity at concentration greater than 0.6 M.

5. Conclusion

Ion exchange behavior of an inorganic ion exchanger depends considerably on the preparation method and the particle size [10]. These behaviors are also observed in this study for cerium(III) molybdate. The thermal gravimetric study suggests that the ion exchange is potentially useful for adsorption of some metal ions at higher temperatures. It was found that because of its high ability to adsorb Cs(I) ion in high ionic strength and in medium acid concentration it can be used for the removal of cesium ions from liquid nuclear wastes. Furthermore, the ion exchange behavior of cerium(III) molybdate demonstrates it to be useful for the separation and analytical purposes such as the uptake of thorium and uranium from neutral or acidic solution as well as separation of some lanthanide metal ions from actinide ones.

References

[1] N. Vajda, C.U. Kim, Determination of radiostrontium isotopes: a review of analytical methodology, Appl. Radiat. Isot. 68 (2010) 2306–2326.
[2] M. Zamorano, A. Grindlay, E. Molero, M.I. Rodríguez, Diagnosis and proposals for waste management in industrial areas in the service sector: case study in the metropolitan area of Granada (Spain), J. Cleaner Prod. 19 (2011) 1946–1955.
[3] M.H. Lee, H.J. Ahn, J.H. Park, Y.J. Park, K. Song, Rapid sequential determination of Pu, ^{90}Sr and ^{241}Am nuclides in environmental samples using an anion exchange and Sr-Spec resins, Appl. Radiat. Isot. 69 (2011) 295–298.
[4] T.H. Woo, H.S. Cho, Nano-scopic measurement for radiation of nuclear waste forms using ion beam injection in the drum treatment, Nucl. Instrum. Met. Phys. Res. A 652 (2011) 69–72.
[5] N. Chubar, New inorganic (an) ion exchangers based on Mg–Al hydrous oxides: (alkoxide-free) sol–gel synthesis and characterisation, J. Colloid Interface Sci. 357 (2011) 198–209.
[6] A.A. Zagorodni, Ion Exchange Materials, Properties and Applications, Elsevier, London, 2007.
[7] R. Thakkar, U. Chudasama, Synthesis and characterization of zirconium titanium phosphate and its application in separation of metal ions, J. Hazard. Mater. 172 (2009) 129–137.
[8] S.A. Nabi, M.N. Inamuddin, Synthesis and characterization of a new inorganic cation-exchanger Zr(IV) tungstomolybdate: analytical applications for metal content determination in real sample and synthetic mixture, J. Hazard. Mater. 142 (2007) 404–411.
[9] A. Zeid, A.O. Inamuddin, M. Naushad, Determination of ion-exchange kinetic parameters for the poly-o-methoxyaniline Zr(IV) molybdate composite cation-exchanger, Chem. Eng. J. 166 (2011) 639–645.
[10] S. Lahiri, K. Roy, S. Bhattacharya, S. Maji, S. Basu, Separation of ^{134}Cs and ^{152}Eu using inorganic ion exchangers, zirconium vanadate and ceric vanadate, Appl. Radiat. Isot. 63 (2005) 293–297.
[11] A. Nilchi, M.R. Hadjmohammadi, S. Rasouli Garmarodi, R. Saberi, Studies on the adsorption behavior of trace amounts of $^{90}Sr^{2+}$, $^{140}La^{3+}$, $^{60}Co^{2+}$, $Ni^{2+}$and Zr^{4+} cations on synthesized inorganic ion exchangers, J. Hazard. Mater. 167 (2009) 531–535.
[12] R. Baron, F.W. Campbell, I. Streeter, L. Xiao, R.G. Compton, Int. J. Electrochem. Sci. 3 (2008) 556.
[13] Q. Zhang, B. Pan, W. Zhang, B. Pan, L.L.X. Wang, J. Wu, X. Tao, Selective removal of Pb(II), Cd(II), and Zn(II) ions from waters by an inorganic exchanger $Zr(HPO_3S)_2$, J. Hazard. Mater. 170 (2009) 824–828.
[14] M.E. Mahmoud, O.F. Hafez, A. Alrefaay, M.M. Osman, Performance evaluation of hybrid inorganic/organic adsorbents in removal and preconcentration of heavy metals from drinking and industrial waste water, Desalination 253 (2010) 9–15.
[15] S. Dhara, S. Sarkar, S. Basu, P. Chattopadhyay, Separation of the ^{90}Sr–^{90}Y pair with cerium(IV) iodotungstate cation exchanger, Appl. Radiat. Isot. 67 (2009) 530–534.
[16] B. Pan, Q. Zhang, W. Du, W. Zhang, B. Pan, Q. Zhang, Z. Xu, Q. Zhang, Selective heavy metals removal from waters by amorphous zirconium phosphate: behavior and mechanism, Water Res. 41 (2007) 3103–3111.
[17] T.S. Jamil, H.S. Ibrahim, I.H.A. El-Maksoud, S.T. El-Wakeel, Application of zeolite prepared from Egyptian kaolin for removal of heavy metals: I. Optimum conditions, Desalination 258 (2010) 34–40.
[18] M. Tsuji, Solid State Ionics 151 (2002) 385–392.
[19] A. Nilchi, B. Maalek, A. Khanchi, M. Ghanadi Maragheh, A. Bagheri, Radiat. Phys. Chem. 75 (2006) 301–308.
[20] F. Rouqureol, J. Rouquerol, K. Sing, Adsorption by Powders and Porous Solids, Academic press, New York, 1980.